

A genome-wide Mendelian randomization study focusing on endoplasmic reticulum stress reveals novel genetic markers for renal cell carcinoma

BINLI GAO¹, ZHAOJUN LI^{2,3}, JIHAN SHI⁴ and JUNWEN SHEN^{2,3}

¹Department of Quality Management, The First Affiliated Hospital of Huzhou Normal University, Huzhou, Zhejiang 313000, P.R. China; ²Department of Urology, The First Affiliated Hospital of Huzhou Normal University, Huzhou, Zhejiang 313000, P.R. China; ³Huzhou Key Laboratory of Precise Diagnosis and Treatment of Urinary Tumors, Huzhou, Zhejiang 313000, P.R. China; ⁴Department of Anesthesiology, Wuxing District People's Hospital and Wuxing District Maternal and Child Health Hospital, Huzhou, Zhejiang 31300, P.R. China

Received October 6, 2025; Accepted May 19, 2026

DOI: 10.3892/ol.2026.15732

Abstract. The causal association between endoplasmic reticulum stress and renal cell carcinoma remains poorly defined. The present study aimed to identify potential causal relationships between endoplasmic reticulum (ER) stress-related genes and renal cell carcinoma (RCC) by integrating multi-omics datasets using summary data-based Mendelian randomization (SMR). Data on the methylation, expression and protein levels of ER stress-related genes were obtained from quantitative trait loci studies. Genetic associations with RCC were derived from 11 studies comprising 5,219 RCC cases of European descent. SMR and colocalization analyses were performed to assess correlations and identify shared causal genetic variants. Molecular experiments were conducted for validation. In total,

1,193 ER stress-related genes were identified. SMR analysis revealed 3 DNA methylation probes (cg07431106, cg12446953 and cg08884395), 1 gene (polycystin 1) and 3 protein probes (SeqId_4125_52, SeqId_3448_13 and SeqId_17161_1) as key causal variants for RCC (SMR, $P < 0.01$; Heterogeneity In Dependent Instruments, $P > 0.01$). Bayesian colocalization analysis corroborated a strong causal relationship for all 7 variables (posterior probability for $H_4 > 0.7$). Multi-omics data integration identified PTEN induced kinase 1 as a protective factor and estrogen receptor 1 as a progression factor in RCC. Molecular experiments demonstrated that ER stress may be a mechanism for RCC progression and sunitinib resistance. The 7 key variables showed significant differences in an RCC cell line model, supporting the SMR results. In conclusion, the results of the present study suggested a potential association between ER stress and RCC. SMR analysis identified 3 cytosine-phosphate-guanine sites, 1 gene and 3 protein sites as causal variants associated with RCC.

Correspondence to: Dr Junwen Shen, Department of Urology, The First Affiliated Hospital of Huzhou Normal University, 158 Square Back Road, Wuxing, Huzhou, Zhejiang 313000, P.R. China
E-mail: wind-301@163.com

Abbreviations: RCC, renal cell carcinoma; GWAS, Genome-Wide Association Studies; eQTL, expression quantitative trait loci; mQTL, methylation quantitative trait loci; pQTL, protein quantitative trait loci; SMR, summary-data-based Mendelian randomization; UPR, unfolded protein response; ER, endoplasmic reticulum; ERS, ER stress; MDSCs, myeloid-derived suppressor cells; SNV, single-nucleotide variant; SNP, single-nucleotide polymorphism; HEIDI, Heterogeneity In Dependent Instruments; OR, odds ratio; TEM, transmission electron microscopy; CpG, cytosine-phosphate-guanine; ccRCC, clear cell RCC; TKI, tyrosine kinase inhibitor; GRP78, glucose-regulated protein 78; IRE1 α , inositol-requiring enzyme 1 α ; ATF6, activating transcription factor 6; CHOP, C/EBP homologous protein; PTEN, phosphatase and tensin homolog; AKT, protein kinase B; ESR1: estrogen receptor 1; ER α , estrogen receptor α ; PINK1, PTEN induced kinase 1

Key words: summary data-based Mendelian randomization, endoplasmic reticulum stress, renal cell carcinoma

Introduction

Renal cell carcinoma (RCC), the most common renal parenchymal epithelial tumor, accounts for 80-95% of all renal cancer cases, according to the World Health Organization 1997 classification (1). Given its global prevalence and substantial mortality, a comprehensive understanding of the etiology, progression and biological characteristics of RCC is crucial for improving prevention, diagnosis and treatment. According to the latest GLOBOCAN 2022 estimates, kidney cancer (including renal pelvis) accounted for 434,419 new cases worldwide, representing 2.2% of all cancer diagnoses and caused 155,702 mortalities (1.6% of all cancer mortalities), ranking it the 14th most common cancer by incidence and 16th by mortality (2). Extended exposure to certain chemicals, industrial pollutants, radiation and other environmental elements, as well as unhealthy habits such as chronic smoking and obesity, can elevate the risk of developing RCC (3). A comprehensive understanding of the factors that contribute to RCC risk is essential for effective prevention and treatment. Researchers have identified genetic mutations, epigenetic

modifications and metabolic reprogramming as key factors strongly associated with RCC occurrence (4).

The treatment of RCC has notably advanced, now including surgical resection, targeted therapy, immunotherapy and combination approaches (5). Current first-line treatments for advanced clear cell (cc)RCC include tyrosine kinase inhibitors (TKIs) such as sunitinib, as well as immune checkpoint inhibitor combinations (6). Despite these advances, acquired resistance to TKIs remains a major clinical challenge. Addressing this resistance requires the development of novel therapeutic strategies informed by a deeper understanding of tumor biology (7). Integrating artificial intelligence into medical informatics can further facilitate precision medicine approaches for RCC treatment (8).

When misfolded or unfolded proteins accumulate in the endoplasmic reticulum (ER) lumen or when calcium ion balance is disrupted, cells activate a series of protective responses known as ER stress. This encompasses signaling pathways involving the unfolded protein response (UPR) to ER overload and the caspase-12-mediated apoptotic pathway (9). To activate protective responses, ER stress induces the upregulation of molecular chaperones within the ER, such as glucose-regulated protein (GRP)78 and GRP94. However, ER stress can also independently trigger internal cell death, ultimately determining the fate of distressed cells, which can range from adaptation to injury or cell death (9).

ER stress plays a dual role in cancer; it can enhance cell survival and inhibit apoptosis by activating signaling pathways such as the UPR. However, excessive or prolonged stress can also induce apoptosis, resulting in cell death. This duality gives ER stress a complex regulatory effect on cancer development. Research indicates that cancer cells activated by inositol-requiring enzyme 1 α (IRE1 α) or PERK-like ER kinase (PERK) can evade detection by natural killer cells and release factors that promote angiogenesis and the recruitment of myeloid-derived suppressor cells (MDSCs) to tumors (10). ER stress-related gene patterns and lectin-like oxidized LDL receptor 1 (LOX1) can differentiate normal neutrophils from polymorphonuclear-MDSCs in patients with cancer, impacting the tumor immune environment (11,12).

ER stress is implicated in RCC, where it can trigger the apoptosis of RCC cells through activation of signaling pathways such as the UPR and PERK/Eukaryotic Initiation Factor 2 (eIF2) (9). However, high expression of ER stress-related proteins, such as GRP78, is also associated with increased tumor invasion and metastasis (13). GRP78/BiP has the ability to enhance the movement and penetration of cancer cells by controlling matrix metalloproteinases and cell adhesion molecules (14). Therefore, researchers speculate that ER stress is an important area of study in RCC development.

Summary-data-based Mendelian randomization (SMR) effectively analyzes the connection between genetic changes and specific phenotypic traits, especially disease susceptibility, by combining genetic and phenotypic data. By leveraging extensive data from Genome-Wide Association Studies (GWAS) and expression quantitative trait loci (eQTL), SMR becomes a powerful tool for uncovering novel disease-associated genes. SMR analysis does not solely concentrate on the statistical correlation between genes and phenotypes; it also endeavors to deduce whether these correlations are causal. By examining

the relationship between gene expression and phenotypes, while controlling for potential confounding factors, SMR provides stronger evidence of causality (15). This method requires integrating multi-omics data, such as genomics and transcriptomics, thereby promoting innovation and advancing biomedical research by introducing new perspectives and approaches to diagnosing and managing complex diseases.

Using the SMR analysis technique along with molecular experiments, the present study examined how ER stress affects RCC progression. The main focus was to pinpoint essential molecules in the ER stress pathway, offering a fresh perspective for RCC prevention and treatment.

Materials and methods

Study design. Fig. 1 contains a comprehensive overview of the research workflow employed in the present study. First, GWAS summary data for different types of RCC were merged with summary data from blood-based eQTL, methylation QTL (mQTL) and protein QTL (pQTL) analyses, then the SMR method was used to identify candidate genes associated with ERS-related gene expression. To further validate these initial findings, Bayesian colocalization analysis were performed. Finally, cell experiments were conducted to corroborate the positive results in renal cancer progression.

Data sources. A comprehensive search was conducted using the GeneCards database (<https://www.genecards.org/>) to identify relevant genes associated with ERS, employing the key word 'endoplasmic reticulum stress' as a guide. Following established protocols, only genes with relevance scores of ≥ 7 were considered for further analysis (16-18). In total, 1,193 ERS-related genes were identified through this process

The blood eQTL and mQTL data were procured utilizing methodologies that have been previously documented in the scientific literature (19-21). The eQTL summary data for genes related to ER stress was obtained from the eQTLGen consortium, a collaborative effort that gathered genetic data pertaining to gene expression from an extensive cohort of 31,684 individuals across 37 diverse datasets (19). Single-nucleotide variant (SNV)-gene pairs that had available data in multiple cohorts and a short genetic distance (≤ 1 Mb) were tested. Relevant information was obtained from the eQTLGen consortium webpage at <https://www.eqtlgen.org/ciseqtl.html>.

Selection criteria and bias control. QTL datasets were selected based on the following: i) Matching European ancestry with RCC GWAS data; ii) sample size $>1,000$; and iii) rigorous quality control in the original studies. Exclusion criteria included: minor allele frequency <0.01 , Hardy-Weinberg equilibrium $P < 0.0001$, call rate <0.95 and platform-specific artifacts. To control for biases, population stratification (multi-dimensional scaling components), batch effects (normalization and probe matching) and cell type composition (surrogate variable analysis) were adjusted for. Linkage disequilibrium confounding were excluded using a Heterogeneity In Dependent Instruments (HEIDI) test ($P > 0.01$) and Bayesian colocalization.

In a study of 35,559 individuals in Iceland, researchers used aptamers to measure plasma protein levels. This analysis

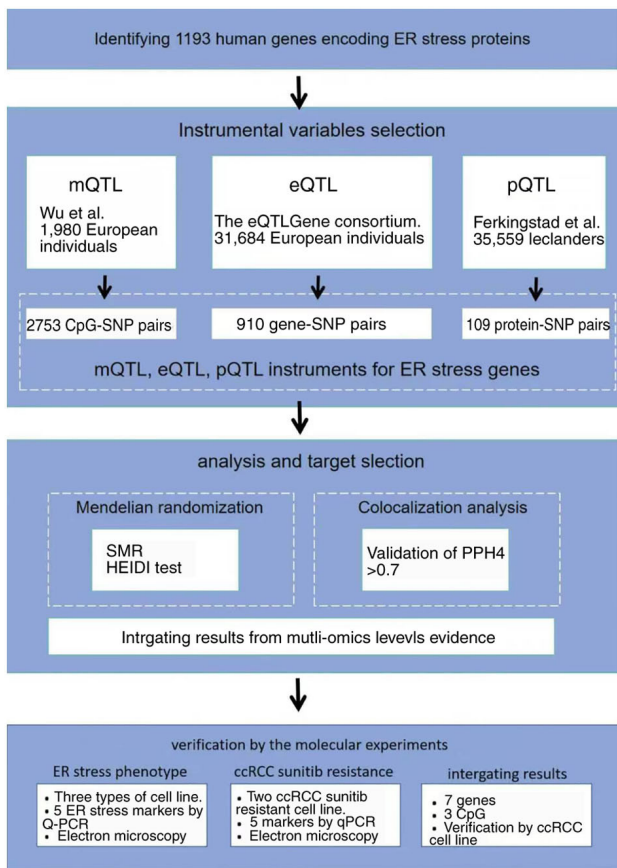


Figure 1. Study design. SMR, summary-based Mendelian randomization; QTL, quantitative trait loci; ES, endoplasmic reticulum; SNP, single nucleotide polymorphisms; PPH4, posterior probability of H4; HEIDI, Heterogeneity In Dependent Instruments; qPCR, quantitative PCR; mQTL, methylation quantitative trait loci; eQTL, expression quantitative trait loci; pQTL, protein quantitative trait loci; CpG, cytosine-phosphate-guanine; ccRCC, clear cell renal cell carcinoma.

identified 4,907 aptamers and associated genetic markers related to protein expression. From this data, 2,364 single-nucleotide polymorphisms (SNPs) potentially influencing the expression of 187 proteins were pinpointed which have been used in the present study (22).

To identify relevant instrumental variables for ERS-related genes, a significance threshold of $P < 5 \times 10^{-8}$ was used. The mQTL summary data were originally from a comprehensive meta-analysis by Wu *et al* (23), and SNV data from the Yang work (23) were downloaded. This meta-analysis incorporated data from two European cohorts, the Lothian Birth Cohorts ($n=1,366$) and the Brisbane Systems Genetics Study ($n=614$) (23). The data were rigorously filtered, retaining only DNA methylation probes with a mQTL significance level of $P < 5 \times 10^{-8}$ and SNVs located within 2 Mb of each DNAm probe. The datasets that were formatted in Biomedical Engineering Standard Data were retrieved from the Specified Medical Resource website (<https://yanglab.westlake.edu.cn/software/smr/#mQTLsummarydata>). The present study centered specifically on the mQTL summaries pertaining to ERS genes.

The dataset (24) comprised two comprehensive scans conducted by the IARC-Centre National de Genotypage, encompassing 11 studies from 18 countries. Specifically, it included 5,219 individuals diagnosed with RCC, consisting

of 1,992 women and 3,227 men as well as 8,011 unaffected individuals (3,095 women and 4,916 men), all of European descent. The first scan used HumanHap 317k, 550 or 610Q arrays for genotyping, while the second scan used Omni5 and OmniExpress arrays (24).

The data used in the present research were obtained from publicly available databases that had already received ethical approval for their original research projects. Therefore, the present study did not require additional ethical clearance.

Mendelian randomization and colocalization. This analytical framework of the present study consisted of two main stages: SMR analysis and a subsequent sensitivity analysis. The SMR analysis formed the basis for the key findings, while the sensitivity analysis was performed to validate the robustness of these results. Detailed descriptions of both the SMR and sensitivity analyses can be found in the Tables SI-SVI.

The initial analysis used a five-step method: i) SNPs as genetic factors, DNAm as the exposure and RCC as the outcome; ii) SNPs as genetic instruments, ER stress-related gene expression as the exposure and RCC as the outcome; iii) SNPs as genetic instruments, ER stress-related protein expression as the exposure and RCC as the outcome; iv) SNPs as genetic factors, DNAm as the exposure and ER stress gene expression as the outcome; and v) SNPs as genetic factors, ER stress-related gene expression as the exposure and protein expression as the outcome. Only findings satisfying the predefined significance thresholds (SMR $P < 0.05$ and HEIDI $P > 0.01$) from the first three steps were selected for further analysis.

To confirm potential causal relationships, the following criteria were used: i) An SMR P value of < 0.05 in all SMR analyses; ii) $P > 0.01$ for HEIDI in all SMR analyses; and iii) verification that the eQTL and mQTL or eQTL and pQTL matched the same gene symbols. Results were measured with odds ratios (ORs) determined by the equation $OR = \exp(\beta \text{ of SMR})$, where β represents the SMR regression coefficient (effect size), indicating the change in log odds of RCC per one standard deviation increase in the exposure trait, and \exp denotes the exponential function (25).

A Bayesian colocalization analysis was performed to determine if a shared causal variant underlies GWAS summary data and different QTLs, specifically eQTLs, pQTLs and mQTLs. This analysis evaluated five primary hypotheses: H0, no association with either GWAS or QTL; H1, association with GWAS only; H2, association with QTL only; H3, association with both GWAS and QTL, but with distinct causal variants; and H4, association with both GWAS and QTL, with a shared causal variant. The posterior probability of each hypothesis was calculated. Following established protocols, all SNVs within 100 kb of the lead SNP associated with the probe were included in the colocalization analysis (26).

To perform colocalization analysis, all SNPs within a 100-kb window flanking the index SNP associated with the probe were identified. PPH4 of > 0.7 was considered as strong evidence of overlap between the GWAS and QTL signals (27).

SMR software version 1.3.1 was used to perform the five-step SMR analysis and the HEIDI test. The 'coloc' R package (version 5.2.2) was used for the co-localization analysis (27). To account for multiple testing in the five-step

SMR analysis, the Benjamini-Hochberg method was applied to correct for potentially incorrect results. $P < 0.05$ was as defined statistical significance in the SMR dataset analysis.

Cell lines and culture. One human proximal tubular epithelial cell line (HK-2; cat. no. GNHu47) and one human embryonic cell line (293T; cat. no. SCSP-502) were used as non-cancerous controls, along with two RCC cell lines (786-O; cat. no. TCHu186; Caki-1, cat. no. TCHu135). All cell lines were obtained from the China Center for Type Culture Collection and cultured in DMEM (Gibco; Thermo Fisher Scientific, Inc.; cat. no. 11875093) containing 10% FBS (Gibco; Thermo Fisher Scientific, Inc.; cat. no. 10099141C) and 1% penicillin-streptomycin-amphotericin B solution (Beyotime Biotechnology; cat. no. C0224-100ml) in an incubator at 37°C with 95% air and 5% CO₂. The cell lines were managed according to the guidelines outlined by the Chinese National Collection of Authenticated Cell Cultures. The HK-2 cell line served as a model of healthy kidney epithelial tissue, whereas the 786-O cell line is derived from ccRCC.

Confluency at the time of experiments was 80-95%. In total, three cell models were established: i) HK-2 cells (normal renal epithelium, control); ii) 293T cells treated with adriamycin (nephropathy model); and iii) 786-O cells (ccRCC). To induce nephropathy, 293T cells were seeded in 6-well plates (2x10⁵ cells/well) and treated with 2 µg/ml adriamycin for 24 h (24).

RNA extraction and reverse transcription-quantitative PCR (RT-qPCR). Total RNA was extracted using TRIzol reagent (Biosharp Life Sciences; cat. no. BS258A). Cells were lysed in 1 ml TRIzol, followed by the addition of 200 µl chloroform. The mixture was then centrifuged at 12,000 x g for 15 min at 4°C. The aqueous phase was collected, mixed with an equal volume of isopropanol, incubated at room temperature for 10 min and centrifuged at 12,000 x g for 10 min at 4°C. The resulting pellet was washed with 70% ethanol, air-dried and resuspended in RNase-free water.

RT was performed using the BeyoRT™ II First Strand cDNA Synthesis Kit (RNase H-) kit (Beyotime Biotechnology; cat. no. D7168S). qPCR was then conducted on an Eppendorf real-time PCR instrument using BeyoFast™ SYBR Green qPCR Mix (Beyotime Biotechnology; cat. no. D7260). The 20 µl reaction contained: 2X SuperMix 10 µl, forward and reverse primers (10 µM) 0.4 µl each, template 2 µl and water 6.8 µl. The thermocycling conditions were as follows: 95°C 3 min; 40 cycles of 95°C 30 sec, 55°C 20 sec and 72°C 20 sec. The relative expression level of target genes was normalized to β-actin as an internal control and calculated using the 2^{-ΔΔC_q} method.

In total, 5 ER stress markers were detected: GRP78, PERK, IRE1α, activating transcription factor 6 (ATF6) and C/EBP homologous protein (CHOP). The primer sequences were as follows (5'-3'): GRP78 (also known as HSPA5) forward GAAAGGATGGTAAATGATGCTGAG and reverse GTC TTCAATGTCCGCATCCTG; PERK forward ACGATGAGA CAGAGTTGCGAC and reverse ATCCAAGGCAGCAAT TCTCCC; IRE1 (also known as ERN1) forward CCGAAC GTGATCCGCTACTTCT and reverse CGCAAAGTCCTT CTGCTCCACA; ATF6 forward TCCCTCGGTCAGTGGA CTCTTA and reverse CTTGGGCTGAATTGAAGGTTT

TG; CHOP forward GGAAACAGAGTGGTCATTCCC and reverse CTGCTTGAGCCGTTTATTCTC; β-actin forward GATGAGATTGGCATGGCTTT and reverse GTCACCTT ACCGTTCCAGT.

To validate the SMR findings, the expression levels of seven key genes [Polycystin 1 (PKD1), C-C Motif Chemokine Ligand 2 (CCL2), PTEN induced kinase 1 (PINK1), estrogen receptor 1 (ESR1), Advanced Glycosylation End-Product Specific Receptor (AGER), Insulin Receptor (INSR), and Dolichyl-Di-N-Acetylglucosamine Phosphodiesterase Alpha-And Beta-Subunits (DDOST)] were quantified. The primer sequences were as follows (5'-3'): PKD1 forward GCCAGA GCGCATAACGAA and reverse TACCCACCACTCACC TCC; CCL2 forward CCAAGCAGAAGTGGGTTCA and reverse GTGTCTGGGGAAAGCTAGGG; PINK1 forward 5'-GCCTCATCGAGGAAAACAGG and reverse GTC TCGTGTCCAACGGGTC; ESR1 forward CCCACTCAA CAGCGTGTCTC and reverse CGTCGATTATCTGAATTT GGCCT; AGER forward GTGTCCTTCCCAACGGCTC and reverse ATTGCCTGGCACC GGAAAA; INSR forward AAA ACGAGGCCCGAAGATTTTC and reverse GAGCCATA GACCCGGAAG; DDOST forward TACGCTCATCGTGGC TGACACT and reverse CCAGCACCAAAGGGTTATCAGG.

Western blot analysis. For ER stress inhibition, cells were pretreated with 4-PBA (2 mM, 24 h, at 37°C in a 5% CO₂ atmosphere; MedChemExpress; cat. no. HY-A2081) prior to protein extraction. Total protein was extracted using RIPA lysis buffer (Beyotime Biotechnology; cat. no. P0013B) supplemented with protease and phosphatase inhibitors (Beyotime Biotechnology; cat. nos. P1005 and P1081). Protein concentration was then determined by BCA assay (Beyotime Biotechnology; cat. no. P0012). Equal amounts of protein (30 µg) were separated by 10% SDS-PAGE and transferred to PVDF membranes (MilliporeSigma; cat. no. IPVH00010). After blocking with 5% non-fat milk in TBST (20 mM Tris-HCl, 150 mM NaCl, 0.1% Tween-20, pH 7.6) for 1 h at room temperature, membranes were incubated overnight at 4°C with primary antibodies against phospho-IRE1α (Affinity Biosciences; cat. no. AF7150; 1:1,000), IRE1α (Cell Signalling Technology, Inc.; cat. no. 3294T; 1:1,000), PERK (Cell Signalling Technology, Inc.; cat. no. 3192S; 1:1,000), phospho-PERK (Affinity Biosciences; cat. no. DF7576; 1:1,000), GRP78 (Abcam; cat. no. ab108613; 1:1,000), CHOP (Cell Signalling Technology, Inc.; cat. no. 2895T; 1:1,000), eIF2α (Cell Signalling Technology, Inc.; cat. no. 5324T; 1:1,000), phospho-eIF2α (Cell Signalling Technology, Inc.; cat. no. 3398T; 1:1,000), ATF6 (Abcam; cat. no. ab227830; 1:1,000) and β-actin (Sigma-Aldrich; Merck KGaA; cat. no. A5316; 1:5,000). After washing with TBST, membranes were incubated with HRP-conjugated anti-rabbit (1:5,000; cat. no. 111-035-144; Jackson ImmunoResearch Laboratories; Inc.) and HRP-conjugated anti-mouse (1:5,000; cat. no. 115-035-146; Jackson ImmunoResearch Laboratories, Inc.) secondary antibodies for 1 h at room temperature. Protein bands were visualized using ECL (cat. no. 1705061; Bio-Rad Laboratories, Inc.) and captured by the ChemiDoc XRS+ system. Densitometric analysis was performed using ImageJ (version 2.16.1; Fiji distribution; National Institutes of Health).

Table I. Primer sequences for methylation-specific PCR analysis.

Primer name	Primer sequence (5'–3')	Product size (bp)
cg12446953-M	F: TTTTATAGTATATTTTATTTTCGT R: TATTTTATAAAAACCAACATTACGTT	172bp
cg12446953-U	F: TTTTATAGTATATTTTATTTTGT R: TATTTTATAAAAACCAACATTACATT	172bp
cg08884395-M	F: AAATTTGTTAGTTGGATTAGATCGA R: TTCAAAAAAACCTTTAATTTAAAACG	184bp
cg08884395-U	F: AAATTTGTTAGTTGGATTAGATTGA R: CAAAAAACCTTTAATTTAAAACACA	182bp
cg07431106-M	F: TTTTGTGAAAAAGGTTTATTTACGT R: CTCCTACTATATACACAACCCTATATTACG	207bp
cg07431106-U	F: ATATAAGTTTTTTGAAAAAGGTTTATTTAT R: CACAACCCTATATTACATA	201bp

F, forward; R, reverse.

Transmission electron microscopy (TEM). Cells were fixed in 2.5% glutaraldehyde overnight at 4°C, post-fixed in 1% osmium tetroxide for 1 h at room temperature, dehydrated in a graded ethanol series (30, 50, 70, 80, 90, 95 and 100% ethanol, 15 min each at room temperature) and embedded in epoxy resin (polymerized at 60°C for 48 h). Ultrathin sections (70 nm) were stained with uranyl acetate for 15 min at room temperature and then with lead citrate for 8 min at room temperature. Images were captured using a JEOL JEM-1010 electron microscope at 80-120 kV. All TEM images were acquired at 500 nm.

Sunitinib resistance. To investigate the role of ERS in sunitinib resistance in ccRCC, sunitinib-sensitive and sunitinib-resistant cell lines were compared using two distinct methods: Western blot analysis of ERS-related protein expression and TEM for ultrastructural observation. Sunitinib-resistant cell lines were developed by exposing ccRCC cells to low doses of sunitinib (cat. no. SU 11248; MedChemExpress).

Methylation-specific PCR (MSP). The methylation status of the genes was determined using MSP. PCR amplification was performed using 150-200 ng of treated DNA as a template, with two primer sets designed for the same target region. One set was specific to methylated DNA at cytosine-phosphate-guanine (CpG) sites and the other to unmethylated DNA. Each 20 µl PCR reaction contained 1 U of Hot start EX Taq DNA polymerase (Takara Bio), 2 µl of 10X EXtaq Buffer, 2 µl of dNTP mixture, 8 pmol each of forward and reverse primer and 1 µl of DNA template. The PCR conditions were as follows: Initial denaturation at 96°C for 3 min, followed by 40 cycles of denaturation at 96°C for 30 sec, annealing at 60°C for 30 sec and extension at 72°C for 30 sec, with a final extension at 72°C for 4 min. PCR products were visualized on either 2% agarose gels or 6% non-denaturing polyacrylamide gels. Primer sequences and expected product sizes are detailed in Table I.

Statistical analysis. Statistical analyses were performed using GraphPad Prism software (version 9.5; Dotmatics).

Data are expressed as mean ± SEM. All experiments were repeated at least three times. Differences between two groups were analyzed using an unpaired two-tailed Student's t-test. For multiple comparisons, one-way or two-way ANOVA followed by Tukey-Kramer's multiple-comparison test was used. Two-way ANOVA was specifically used to analyze data involving two independent variables, such as cell type and drug treatment condition. P<0.05 was considered to indicate a statistically significant difference.

Results

Statistical analysis of genetic variants and trait associations using SMR on mQTL and GWAS datasets. SMR was employed to investigate the relationship between SNVs, DNA methylation sites and ERS-related genes. Using blood mQTL data, 4,234 CpG sites associated with 1,193 ERS-related genes were identified, which were linked to 64,238 SNPs (Table SI).

Subsequently, the mQTL information for ERS genes was integrated with the GWAS results for RCC. This integration identified 3 DNA methylation probes (cg07431106, cg12446953 and cg08884395) corresponding to 3 ER stress-related genes (CCL2, PINK1 and ESR1), with SMR P<0.01 and HEIDI P<0.01 (Fig. 2). Causality estimates are expressed as β-values, representing the effect size for a one standard deviation change in ER stress-associated gene expression levels. Additionally, 2 protective associations between methylation levels and RCC (cg07431106, β=-0.18; cg12446953, β=-0.544) and 1 progression association suggesting increased risk of RCC (cg08884395, β=0.563) were observed.

Statistical analysis of genetic variation for eQTL and GWAS datasets. Analysis of eQTL data revealed 985 eQTL probes linked to ERS genes, which were connected to 15,618 SNPs (Table SII). Integration of the eQTL data with the RCC GWAS data identified 834 ERS-related genes. One gene (PKD1) demonstrated a protective effect against RCC (Fig. 2), with a β-value of -1.44 (SMR, P< 0.001; HEIDI, P=0.836).

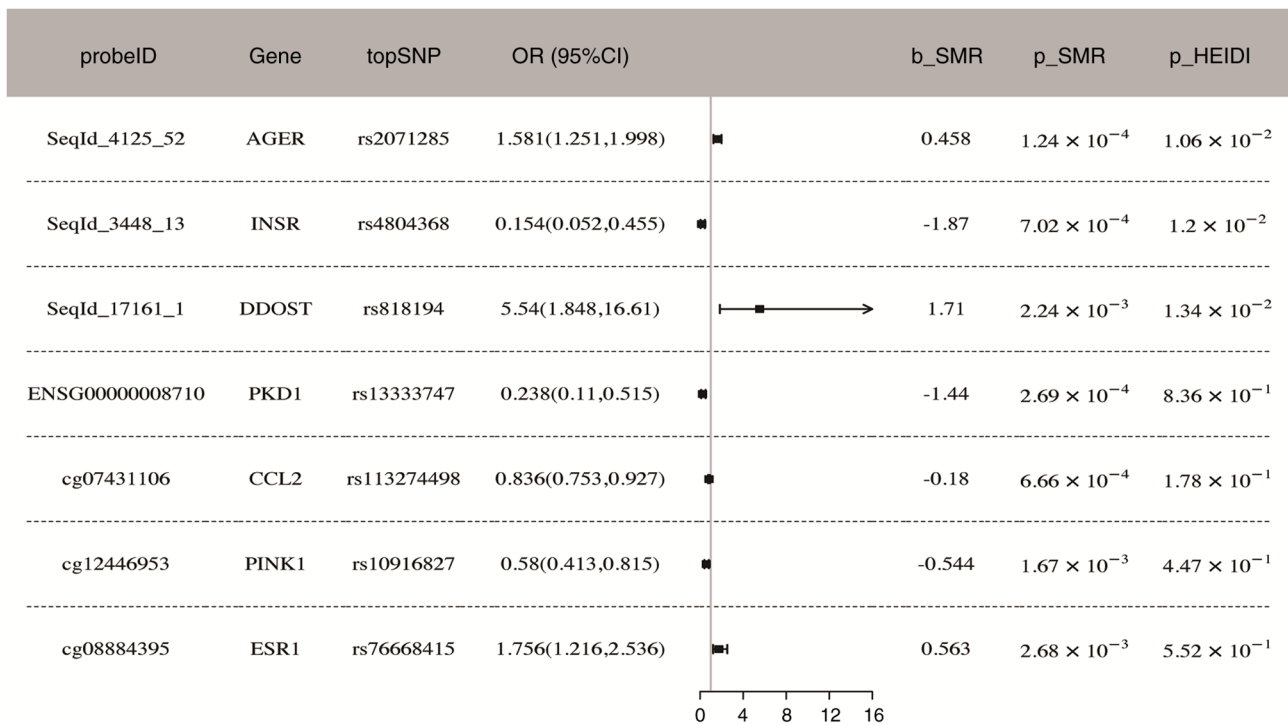


Figure 2. Associations of genetically predicted ER stress-related molecular features with renal cell carcinoma in Mendelian randomization analysis. DNA methylation probes (mQTL): cg07431106 (CCL2), cg12446953 (PINK1) and cg08884395 (ESR1). Gene expression (eQTL): PKD1. Protein probes (pQTL): SeqId_4125_52 (AGER), SeqId_3448_13 (INSR) and SeqId_17161_1 (DDOST). b_SMR, the β -value of SMR; p_SMR, the P-value of SMR; OR, odds ratio; CI, confidence interval; p_HEIDI, the P-value of the HEIDI analysis. AGER, advanced glycosylation end-product specific receptor; INSR, insulin receptor; DDOST, dolichyl-di-N-acetylglucosamine phosphodiesterase alpha- and beta-subunits; PKD1, polycystin 1; CCL2, C-C motif chemokine ligand 2; PINK1, PTEN induced kinase 1; ESR1, estrogen receptor 1.

MR analysis for pQTL and RCC outcomes. In total, 187 potential pQTL tools related to genetic variations were identified, suggesting a connection between the levels of 175 proteins and the risk of RCC (Table SIII). Specifically, integrating pQTL data with RCC GWAS summary data identified 3 protein probes (SeqId_4125_52, SeqId_3448_13 and SeqId_17161_1) corresponding to 3 ERS-related genes (AGER, INSR and DDOST). These probes exhibited significant associations with RCC risk (SMR, $P < 0.01$; HEIDI, $P > 0.01$; Fig. 2). Probe SeqId_17161_1 demonstrated the strongest cancer-promoting effect ($\beta = 1.71$). Probe SeqId_4125_52 also promoted cancer progression ($\beta = 0.458$), whereas probe SeqId_3448_13 acted as a protective factor against kidney cancer ($\beta = -1.87$). Sensitivity, heterogeneity and multi-effect analysis results are presented in Tables SIV, SV and SVI, respectively.

Bayesian co-localization analysis. Bayesian co-localization analysis was used to eliminate potential confounding variables associated with RCC. The results indicated that 7 variants shared a causal relationship with RCC: 3 DNA methylation CpG sites (cg07431106, PPH4=0.786; cg12446953, PPH4=0.813; cg08884395, PPH4=0.915), 1 gene (PKD1, PPH4=0.944) and 3 proteins (AGER, PPH4=0.901; INSR, PPH4=0.875; DDOST, PPH4=0.738) (Fig. 3).

SMR analysis for eQTL and mQTL data. Given the well-known influence of gene methylation on gene expression, the potential association between DNA methylation and gene expression was investigated. Specifically, DNA methylation was used

as the predictor variable and gene transcripts as the response variable. Using strict criteria (SMR FDR < 0.05 and HEIDI $P > 0.01$), specific regulatory connections were identified where the activity of 2 genes related to ER stress were influenced by 10 CpG sites associated with DNA methylation. For example, 2 methylation sites (cg01961278 and cg17183232) were significantly associated with PINK1 expression and positively correlated with it. For ESR1, 8 methylation sites (cg15626350, cg00601836, cg04063345, cg21157690, cg04211581, cg17264271, cg24764793 and cg06611115) exhibited varying regulatory effects on ESR1 expression (Tables SII and SIII).

SMR analysis for eQTL and pQTL data. Using the same screening criteria (SMR FDR < 0.05 and HEIDI $P > 0.01$), no regulatory relationships between ERS-related proteins and genes were identified (Tables SII and SIII).

ERS drives ccRCC development. Additional molecular tests confirmed that ER stress may play a crucial role in ccRCC progression. Based on three cell models (ccRCC, human embryonic kidney-derived cells treated with adriamycin as a general cellular stress control and renal epithelial cell lines), the level of ER stress increased with disease progression (ccRCC cell lines $>$ human embryonic kidney $>$ renal epithelial cell lines). The levels of 5 ER stress-related molecules (GRP78, PERK, IRE1 α , ATF6 and CHOP) were highest in the ccRCC cell line and lowest in the renal epithelial cell line ($P < 0.01$; Fig. 4A). TEM analysis revealed progressive ultra-structural alterations characteristic of ER stress, including

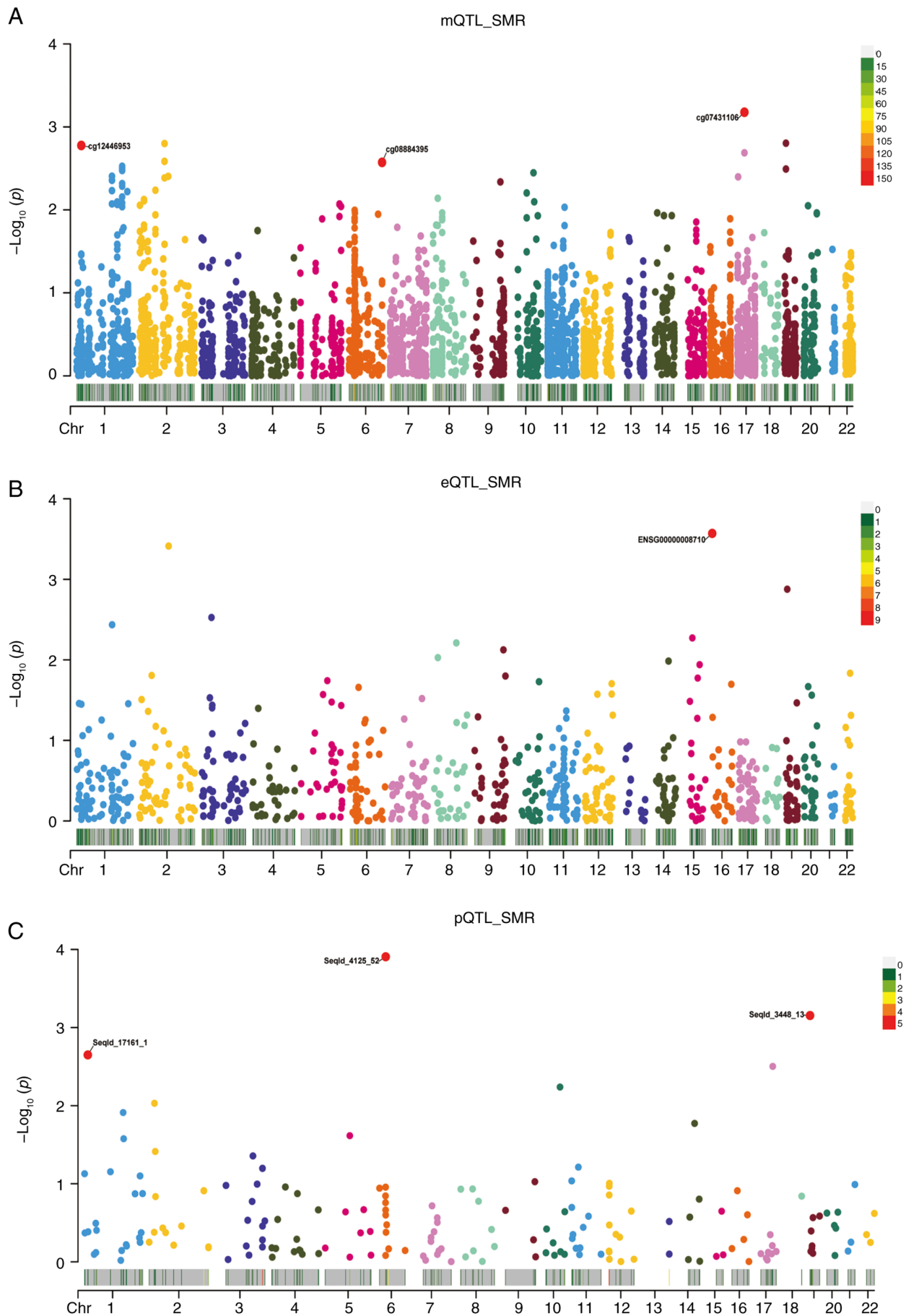


Figure 3. Manhattan plot of the associations between ER stress gene molecular features and renal cell carcinoma. Manhattan plot for ER stress gene (A) methylation, (B) expression and (C) protein abundance. Genes with significant signals in protein abundance levels were labeled. SMR, summary-data-based Mendelian randomization; mQTL, methylation quantitative trait loci; eQTL, expression quantitative trait loci; pQTL, protein quantitative trait loci.

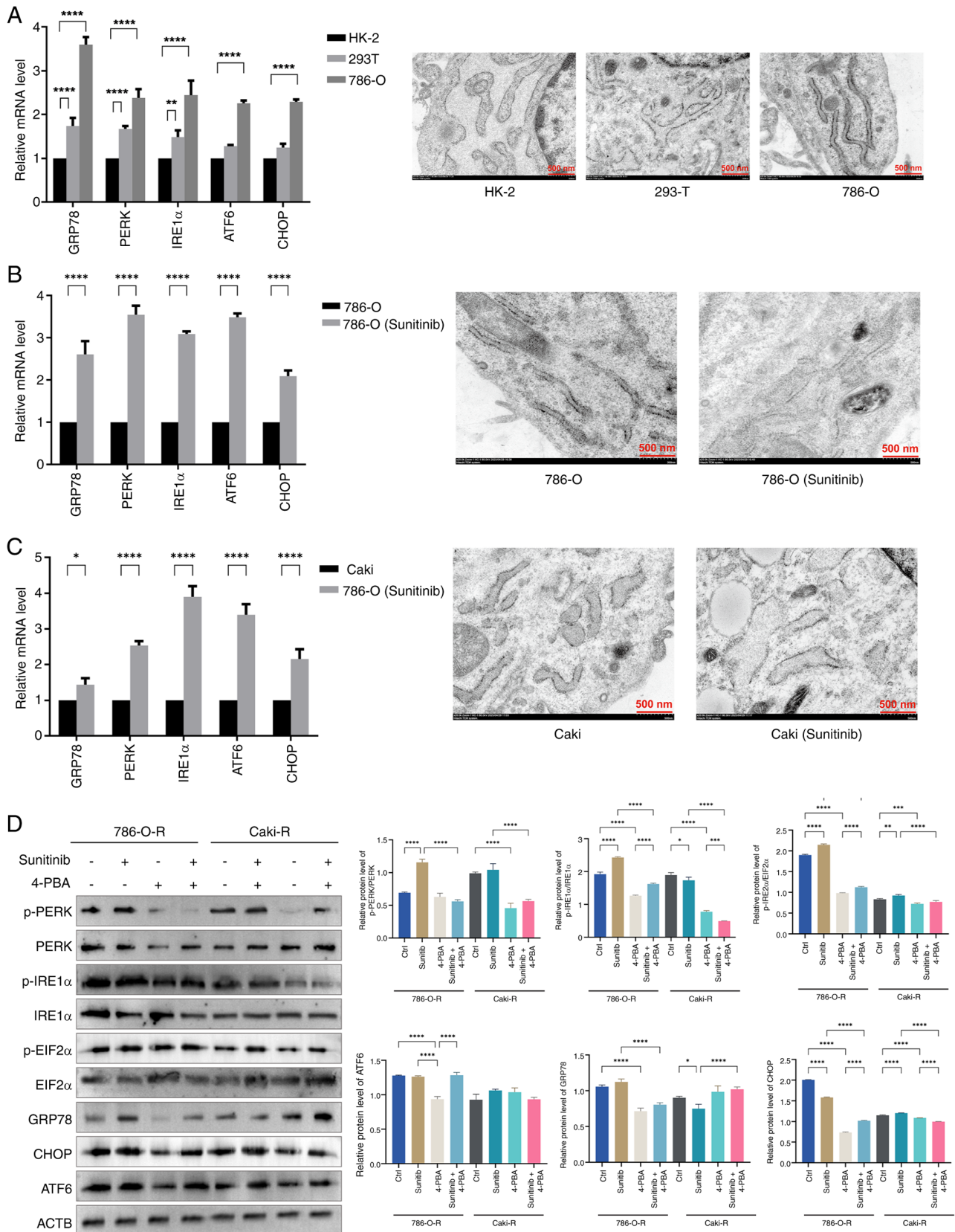


Figure 4. ER stress induces RCC development and resistance to sunitinib. (A) qPCR (left) and TEM (right) confirming ER stress induction in RCC development. In total, 3 cell line models were used: HK-2 (normal renal epithelial cells), 293T with adriamycin (nephropathy model) and 786-O (clear cell RCC). qPCR markers for ER stress included GRP78, PERK, IRE1 α , ATF6 and CHOP. TEM scale bar, 500 nm scale. The levels of ER stress markers are higher in sunitinib resistant (B) 786-O and (C) Caki-1 cells. ER stress phenotype was verified by qPCR (left) and TEM (right, 500 nm scale). (D) Western blot analysis of ER stress markers (p-PERK, PERK, p-IRE1 α , IRE1 α , p-eIF2 α , eIF2 α , GRP78, CHOP and ATF6) in 786-O and Caki-1 cell lines with or without sunitinib resistance, showing activation of ER stress pathways. ACTB served as the loading control. Treatment with 4-PBA (ER stress inhibitor) was included as an experimental control. * $P < 0.05$, ** $P < 0.01$, *** $P < 0.001$, **** $P < 0.0001$. ER, endoplasmic reticulum; TEM, transmission electron microscopy; RCC, renal cell carcinoma; qPCR, quantitative PCR; GRP78, glucose-regulated protein 78; PERK, protein kinase R-like endoplasmic reticulum kinase; IRE1 α , inositol-requiring enzyme 1 α ; ATF6, activating transcription factor 6; CHOP, C/EBP homologous protein; ACTB, actin beta; p-, phosphorylated.

ER swelling, dilatation and vacuolization, which were most pronounced in 786-O cells, moderate in adriamycin-treated 293T cells, and minimal in HK-2 cells (Fig. 4A).

ERS contributes to sunitinib resistance in ccRCC. The potential importance of ER stress in ccRCC resistance to sunitinib was investigated by studying two sunitinib-resistant ccRCC cell lines [786-O (sunitinib) and Caki (sunitinib)] and comparing them with sensitive cell lines. Both resistant cell lines exhibited increased expression of 5 genes (GRP78, PERK, IRE1 α , ATF6 and CHOP) related to ER stress. TEM analysis confirmed these findings by showing marked ER dilatation and swelling in sunitinib-resistant cells compared to their sensitive counterparts, indicating enhanced ER stress in the resistant phenotype (Fig. 4B and C).

To explore the role of ER stress in sunitinib resistance in ccRCC, the ER stress inhibitor 4-PBA was introduced and western blotting was used to assess 5 ER stress markers (GRP78, PERK, IRE1 α , ATF6 and CHOP) in the sunitinib-resistant and sensitive ccRCC cell lines. The results showed that these ER stress markers were significantly higher in sunitinib-resistant ccRCC cell lines than in sensitive cell lines. After 4-PBA intervention, the half-maximal inhibitory concentration of sunitinib was markedly decreased in both sunitinib-resistant RCC cell lines; the IC₅₀ value of the 786-O resistant strain decreased from 24.67 to 13.22 μ M, and the IC₅₀ value of the Caki-1 resistant strain decreased from 16.79 to 9.76 μ M (Fig. S1). Simultaneously, the expression of the ER stress-related proteins in resistant cell lines decreased markedly when treated with 4-PBA compared with the sunitinib-treated group. Specifically, the phosphorylation of PERK and IRE1 α , and downstream effectors such as CHOP, were markedly reduced when treated with 4-PBA compared with sunitinib-treated group. Additionally, the levels of GRP78 and ATF6 declined, indicating that 4-PBA effectively inhibited the ER stress response (Fig. 4D) when treated with 4-PBA compared with sunitinib-treated group.

Molecular experiments validate the expression levels of methylation sites and genes in ccRCC cell lines. The expression levels of 7 key genes, CCL2 (cg07431106), ESR1 (cg08884395), PINK1 (cg12446953), PKD1 (ENSG00000008710), AGER (SeqId_4125_52), INSR (SeqId_3448_13) and DDOST (SeqId_17161_1), selected through SMR analysis, were focused on in this analysis. Comparing the expression levels of these 7 genes across the three cell models revealed significant differences ($P < 0.05$; Fig. 5A), indicating differential expression. Specifically, compared with normal renal HK-2 and 293T cells, the expression levels of all 7 molecules were upregulated in 786-O cells, with the highest expression levels observed in ccRCC cells, suggesting a positive correlation between the degree of ER stress and ccRCC. Furthermore, the methylation levels of three key methylation sites (cg07431106, cg08884395 and cg12446953) in the ccRCC (786-O cell line), human embryonic kidney (293T cell line) and renal epithelial (HK2 cell line) cell models were analyzed. The results suggested that cg0743110 showed methylation characteristics in ccRCC cells but demethylation characteristics in nephropathy and renal epithelial cell models. Site cg08884395 showed methylation characteristics in the nephropathy model

but demethylation characteristics in ccRCC or renal epithelial cell models. Site cg12446953 showed methylation characteristics in ccRCC or renal epithelial cell models but demethylation characteristics in the nephropathy model (Fig. 5B).

Discussion

Using MR and colocalization analyses, the present study investigated potential relationships between the genetically predicted methylation, expression and protein levels of ER stress genes and RCC. The results suggested a possible association between the PKD1 gene and RCC. Additionally, three DNA methylation probes (cg07431106, cg12446953 and cg08884395) corresponding to the ER stress-related genes CCL2, PINK1 and ESR1 were identified. Furthermore, three protein probes (SeqId_4125_52, SeqId_3448_13 and SeqId_17161_1) corresponding to the ER stress-related genes AGER, INSR and DDOST were also shown to be associated with RCC. Bayesian colocalization analysis revealed that all 7 variables shared genetic variants with RCC, further supporting the importance of these factors in renal cancer progression. SMR analysis, combining eQTL and mQTL data, confirmed the involvement of 2 ER stress genes, PINK1 and ESR1. PINK1 expression was regulated by 2 methylation sites, while ESR1 expression was regulated by 8, suggesting that the effects of these genes on renal cancer progression may be controlled by both DNA methylation and gene transcription levels. These findings highlight the molecular mechanisms through which ER stress influences renal cancer progression.

PINK1, a serine/threonine kinase, is critical for maintaining mitochondrial homeostasis. In RCC, mitochondrial dysfunction is a characteristic consequence of von Hippel-Lindau (VHL) loss and pseudohypoxia. PINK1-mediated mitophagy may have a dual role: i) Protective, by clearing damaged mitochondria to limit reactive oxygen species and prevent Hypoxia-inducible factor- α (HIF- α) stabilization; and ii) tumor-promoting, by maintaining mitochondrial function to support the energy demands of hypoxic ccRCC cells (28). The present finding that cg12446953 methylation, which is associated with reduced PINK1 expression, is protective suggests that suppressing PINK1 may disrupt mitochondrial adaptation in RCC, thereby promoting cell death. In the present study, PINK1 expression was elevated in ccRCC cells, supporting its role in tumor maintenance. PINK1 interacts with phosphatase and tensin homolog (PTEN) at serine 179, activating protein kinase B (AKT) and suppressing PTEN nuclear translocation (29), thereby promoting survival pathways commonly activated in RCC. By regulating PTEN and other pathways, PINK1 participates in promoting cancer metastasis. For example, PINK1 suppression can prevent the spread of tumors to the abdomen and reduce resistance to chemotherapy in ovarian cancer (30).

The ESR1 gene encodes estrogen receptor α (ER α), a key regulator in various tissues, particularly hormone-sensitive tissues such as the breast and uterus. Although RCC has traditionally been considered non-hormone dependent, emerging evidence suggests sex-specific differences in incidence and prognosis. Furthermore, ESR1 polymorphisms appear to be associated with RCC risk (31). In the present study, cg08884395 methylation (linked to ESR1) showed an association with RCC

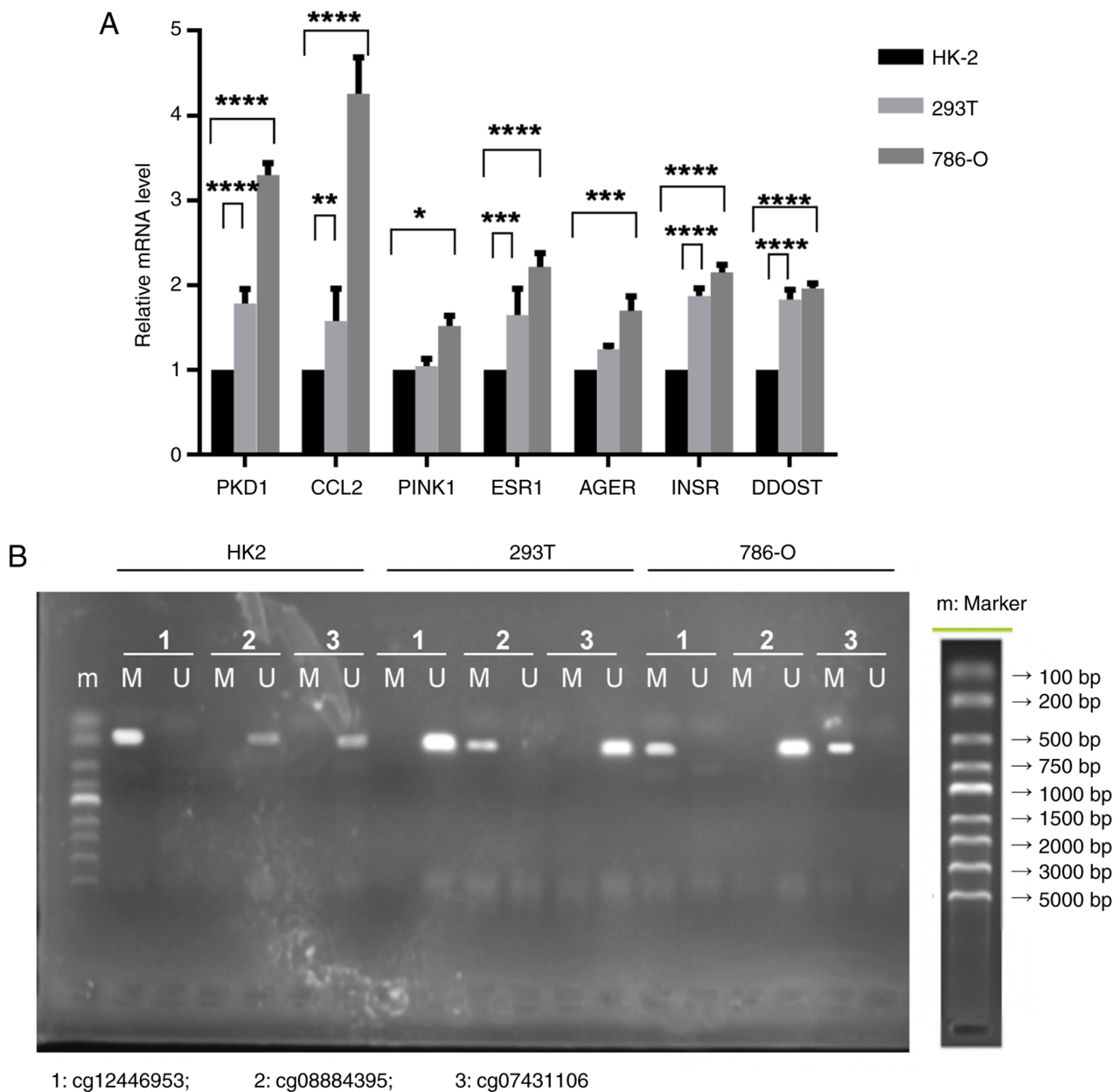


Figure 5. Expression levels of 3 methylation sites and 7 genes were verified in a ccRCC cell line. (A) Expression analysis of 7 ER stress-related genes (CCL2, ESR1, PINK1, PKD1, AGER, INSR and DDOST) in renal related cell lines (HK2, 293T and 786-0) showing significant upregulation. (B) Methylation status of 3 key CpG sites (cg07431106, cg08884395 and cg12446953) in different cell models. cg07431106 showed methylation characteristics specific to ccRCC cells, cg08884395 to nephropathy models and cg12446953 to both ccRCC and renal epithelial cell models. * $P < 0.05$, ** $P < 0.01$, *** $P < 0.001$, **** $P < 0.0001$. ER, endoplasmic reticulum; ccRCC, clear cell renal cell carcinoma; CpG, cytosine-phosphate-guanine; CCL2, C-C motif chemokine ligand 2; ESR1, estrogen receptor 1; PINK1, PTEN induced kinase 1; PKD1, polycystin 1; AGER, advanced glycosylation end-product specific receptor; INSR, insulin receptor; DDOST, dolichyl-di-N-acetylglucosamine phosphodiesterase alpha- and beta-subunits; M, methylated; U, unmethylated.

progression ($\beta = 0.563$), suggesting that epigenetic dysregulation of ESR1 may promote RCC. Potential mechanisms for this include: i) Direct transcriptional activation of proliferation genes (such as Cyclin D1) (30); ii) cross-talk with hypoxia signaling. ER α may stabilize HIF- α independently of VHL, accelerating glycolytic adaptation in ccRCC; and iii) immune modulation. Estrogen signaling affects tumor-infiltrating lymphocytes, which are critical for the RCC immunotherapy response (29). The concurrent upregulation of ESR1 in ccRCC cells and distinct methylation pattern observed in the present study suggest a tumor-promoting role, contrasting with its established function in breast cancer. In breast cancer,

ESR1 encodes estrogen receptor α (ER α), which generally exerts tumor-suppressive effects; ESR1 downregulation or mutation is associated with aggressive disease, poor prognosis and resistance to endocrine therapy (31).

In RCC, ER stress exhibits context-dependent effects mediated by the three UPR pathways. The PERK/eIF2 α /ATF4 pathway initially promotes cell survival by reducing protein synthesis and initiating autophagy. However, prolonged activation of this pathway triggers CHOP-mediated apoptosis. Specifically, in ccRCC, VHL loss leads to constitutive HIF- α activation, increasing the protein synthesis load and inducing ER stress. Adaptive UPR activation enables tumor cells to

withstand this metabolic stress (32). Conversely, pharmacologically induced ER stress can push cells toward apoptosis. This dual functionality creates a therapeutic opportunity. That is, targeting the adaptive phase of the UPR may selectively eliminate RCC cells that rely on this survival mechanism.

In tumor cells, ER stress reshapes the tumor microenvironment by stimulating the secretion of VEGF and IL-6, which in turn promotes angiogenesis and the recruitment of MDSCs (9). In the present study, elevated levels of ER stress markers were observed in sunitinib-resistant RCC cell lines, indicating that therapeutic stress may induce an adaptive UPR that facilitates survival under drug pressure. Mechanistically, previous a study has demonstrated that PERK-mediated upregulation of ATF4 activated amino acid biosynthesis, while IRE1 α -XBP1 splicing enhanced lipid synthesis, leading to membrane remodeling (9). In the present study, treatment with the ER stress inhibitor 4-PBA resensitized resistant cells to sunitinib, supporting this mechanism as a potential therapeutic target

The mechanistic discussion has been focused on PINK1 and ESR1, 2 of the 7 identified variants, as integrated mQTL and eQTL analyses statistically linked their methylation to their expression, they represent distinct functional categories relevant to cancer and their methylation status were experimentally validated in cellular models. The remaining 5 genes (CCL2, PKD1, AGER, INSR and DDOST) were identified through single-omics layers (mQTL for CCL2; eQTL for PKD1; pQTL for AGER, INSR and DDOST) and their specific roles in ER stress-mediated RCC progression require further investigation.

In the present study, concurrent upregulation of both protective factors (such as PINK1 and PKD1) and promoting factors (such as SeqId_17161_1, SeqId_4125_52, ESR1, and DDOST) was observed in ccRCC cell lines, highlighting the complexity and intratumoral heterogeneity of the tumor microenvironment. Elevated expression of protective factors may reflect inherent cellular defense mechanisms against tumor progression, potentially inhibiting malignancy through cell cycle regulation, suppression of proliferation, or induction of apoptosis. Conversely, upregulation of promoting factors may represent adaptive changes that facilitate tumor cell survival and proliferation within an unfavorable microenvironment (13,31). This differential dependency on ER stress pathways across subclones, for instance, PINK1-high cells relying on mitophagy for survival under hypoxic conditions, whereas ESR1-high cells proliferating through PI3K/AKT activation (9), explains why broad ER stress targeting (such as 4-PBA) can be effective, whereas inhibitors targeting single pathways may not. Single-cell analysis is therefore necessary to map these distinct ER stress states and to inform rational combination therapy strategies (33).

To systematically identify potential ERS-related targets in RCC, the present study used SMR analysis, integrating multi-omics data (eQTL, mQTL and pQTL). Although this approach yielded numerous candidate genes and molecular markers, these findings are based on correlation analysis and require systematic experimental validation to confirm their biological functions and causal relationships. To address these limitations, future research should focus on experimentally validating the potential targets identified in the present study to fully elucidate their functional mechanisms.

The present study has several limitations. First, eQTL and mQTL data were derived from blood, not renal tissue. Although blood QTLs can capture systemic regulation, they may not fully represent kidney-specific mechanisms. However, moderate correlations ($r=0.6-0.8$) between blood and kidney eQTLs have been reported for a number of genes (34), and RCC involves systemic immune and metabolic dysregulation. Second, to match available GWAS data, the analysis was restricted to individuals of European ancestry, which limits the generalizability of the findings to other populations. Third, despite using rigorous statistical methods such as Bayesian colocalization, residual confounding from linkage disequilibrium and pleiotropic effects (such as the dual roles of PINK1 in apoptosis inhibition and drug resistance) could affect the accuracy of the causal inferences. Fourth, although statistically significant molecular markers (such as cg07431106 methylation site and AGER protein) were identified, their specific biological mechanisms in RCC development require experimental validation through systematic functional studies. Fifth, inherent differences between cell-based models and the complex *in vivo* tumor microenvironment limit the ability to fully replicate human pathophysiology. Finally, the clinical relevance of the identified potential biomarkers needs further validation in prospective clinical cohorts. These limitations underscore the need for future research incorporating kidney-specific multi-omics data (such as from the Kidney Precision Medicine Project), more physiologically relevant experimental models, multi-ethnic validation and clinical translation studies to improve the understanding of the role of ER stress in RCC progression.

The 7 biomarkers (3 CpG sites: cg07431106, cg12446953 and cg08884395; 1 gene: PKD1; 3 proteins: AGER, INSR and DDOST) identified in the present study have potential for clinical translation. First, methylation markers in blood DNA could serve as non-invasive, early diagnostic tools for RCC screening, especially in high-risk populations. Second, protein markers (AGER, INSR and DDOST) could inform risk stratification and the selection of targeted therapies. Third, since ESR1 methylation is reversible, demethylating agents may have therapeutic potential in RCC subtypes with specific ER stress profiles.

Validation in prospective cohorts is needed to: i) Confirm biomarker performance in multi-ethnic populations; ii) assess longitudinal changes in biomarker levels during disease progression and therapy; and iii) evaluate how these biomarkers integrate with existing clinical scores (such as the International Metastatic Renal Cell Carcinoma Database Consortium criteria). Future studies should also explore combination strategies that target ER stress pathways (such as 4-PBA with TKIs) to overcome drug resistance. In summary, experimental validation of methylation-expression causality will be pursued in subsequent research.

In conclusion, the results of the present study support a potential association between ER stress and RCC. Specifically, SMR analysis identified 3 CpG probes (cg07431106, cg08884395 and cg12446953), 1 gene (PKD1) and 3 protein probes (SeqId_4125_52, SeqId_3448_13 and SeqId_17161_1) associated with RCC progression. For clinical translation, these blood-based methylation markers may aid early diagnosis, the protein markers may enable risk stratification and

demethylating agents could target ESR1-methylated tumors. A validation roadmap has been proposed, including examining multi-ethnic cohorts, longitudinal monitoring and integration with clinical scores. Therapeutically, combining ER stress-targeted agents (such as 4-PBA) with TKIs may overcome resistance. Collectively, these findings provide a basis for biomarker-guided diagnosis and ER stress-focused therapy in RCC.

Acknowledgements

Not applicable.

Funding

This study was financially supported by Public Welfare Projects of the Huzhou Science and Technology Bureau (grant no. 2024GZ84), Zhejiang Provincial Clinical Research Program of Traditional Chinese Medicine (grant no. 2026ZL0842) and the Medicine and Health Program of Zhejiang province (grant no. WKJ-ZJ-26091).

Availability of data and materials

The data generated in the present study may be requested from the corresponding author.

Authors' contributions

BG drafted the manuscript. JuS revised the whole manuscript. ZL and JiS performed bioinformatic analysis and prepared all figures. ZL and JiS confirm the authenticity of all the raw data used in this study. BG, JuS, ZL and JiS participated in laboratory experiments. All authors read and approved the final version of the manuscript.

Ethics approval and consent to participate

Not applicable.

Patient consent for publication

Not applicable.

Competing interests

The authors declare that they have no competing interests.

References

- McGregor BA and Choueiri TK: Renal cell cancer. *Hematol Oncol Clin North Am* 37: xvii-xix, 2023.
- Bray F, Laversanne M, Sung H, Ferlay J, Siegel RL, Soerjomataram I and Jemal A: Global cancer statistics 2022: GLOBOCAN estimates of incidence and mortality worldwide for 36 cancers in 185 countries. *CA Cancer J Clin* 74: 229-263, 2024.
- Campbell SC, Clark PE, Chang SS, Karam JA, Souter L and Uzzo RG: Renal mass and localized renal cancer: Evaluation, management, and follow-up: AUA guideline: Part I. *J Urol* 206: 199-208, 2021.
- Chakraborty S, Balan M, Sabarwal A, Choueiri TK and Pal S: Metabolic reprogramming in renal cancer: Events of a metabolic disease. *Biochim Biophys Acta Rev Cancer* 1876: 188559, 2021.
- Haggstrom LS, Chan WY, Nagrial A, Chantrill LA, Sim HW, Yip D and Chin V: Chemotherapy and radiotherapy for advanced pancreatic cancer. *Cochrane Database Syst Rev* 12: CD011044, 2024.
- Gao S, Ye K, Zhang Z, Wang W, Li J, Xu T and Tan H: Polysaccharides of *pseudostellaria heterophylla* (Miq.) pax et hoffm: Extraction, purification, structural characteristics, pharmacological activities, and structure-activity relationships: A review. *Int J Biol Macromol* 330: 148082, 2025.
- Girnyi S, Marano L, Skokowski J, Mocarski P, Kyclyer W, Gallo G, Dyzmann-Sroka A, Kazmierczak-Siedlecka K, Kalinowski L, Banasiewicz T and Polom K: Prehabilitation approaches for gastrointestinal cancer surgery: A narrative review. *Rep Pract Oncol Radiother* 29: 614-626, 2024.
- Jiang Y, Wang C, Zu C, Rong X, Yu Q and Jiang J: Synergistic potential of nanomedicine in prostate cancer immunotherapy: Breakthroughs and prospects. *Int J Nanomedicine* 19: 9459-9486, 2024.
- Chen X and Cubillos-Ruiz JR: Endoplasmic reticulum stress signals in the tumour and its microenvironment. *Nat Rev Cancer* 21: 71-88, 2021.
- Okubo K, Sato A, Isono M, Asano T and Asano T: Nelfinavir induces endoplasmic reticulum stress and sensitizes renal cancer cells to TRAIL. *Anticancer Res* 38: 4505-4514, 2018.
- Saaoud F, Liu L, Xu K, Cueto R, Shao Y, Lu Y, Sun Y, Snyder NW, Wu S, Yang L, *et al*: Aorta- and liver-generated TMAO enhances trained immunity for increased inflammation via ER stress/mitochondrial ROS/glycolysis pathways. *JCI Insight* 8: e158183, 2023.
- Wu CF, Hung TT, Su YC, Chen PJ, Lai KH and Wang CC: Endoplasmic reticulum stress of oral squamous cell carcinoma induces immunosuppression of neutrophils. *Front Oncol* 12: 818192, 2022.
- Pham HHT, Seong YA, Ngabire D, Oh CW and Kim GD: *Cyperus amuricus* induces G1 arrest and apoptosis through endoplasmic reticulum stress and mitochondrial signaling in human hepatocellular carcinoma Hep3B cells. *J Ethnopharmacol* 208: 157-164, 2017.
- Bai Y, Wei Y, Wu L, Wei J, Wang X and Bai Y: C/EBP β mediates endoplasmic reticulum stress regulated inflammatory response and extracellular matrix degradation in LPS-stimulated human periodontal ligament cells. *Int J Mol Sci* 17: 385, 2016.
- Krishnamoorthy S, Li GH and Cheung CL: Transcriptome-wide summary data-based mendelian randomization analysis reveals 38 novel genes associated with severe COVID-19. *J Med Virol* 95: e28162, 2023.
- Zhang Q, Guan G, Cheng P, Cheng W, Yang L and Wu A: Characterization of an endoplasmic reticulum stress-related signature to evaluate immune features and predict prognosis in glioma. *J Cell Mol Med* 25: 3870-3884, 2021.
- Liang X, Han M, Zhang X, Sun X, Yu K, Liu C, Zhang J, Hu C and Zhang J: Dahuang danshen decoction inhibits pancreatic fibrosis by regulating oxidative stress and endoplasmic reticulum stress. *Evid Based Complement Alternat Med* 2021: 6629729, 2021.
- Xu S, Li X, Zhang S, Qi C, Zhang Z, Ma R, Xiang L, Chen L, Zhu Y, Tang C, *et al*: Oxidative stress gene expression, DNA methylation, and gut microbiota interaction trigger Crohn's disease: A multi-omics Mendelian randomization study. *BMC Med* 21: 179, 2023.
- Vösa U, Claringbould A, Westra HJ, Bonder MJ, Deelen P, Zeng B, Kirsten H, Saha A, Kreuzhuber R, Yazar S, *et al*: Large-scale cis- and trans-eQTL analyses identify thousands of genetic loci and polygenic scores that regulate blood gene expression. *Nat Genet* 53: 1300-1310, 2021.
- McRae AF, Marioni RE, Shah S, Yang J, Powell JE, Harris SE, Gibson J, Henders AK, Bowdler L, Painter JN, *et al*: Identification of 55,000 replicated DNA methylation QTL. *Sci Rep* 8: 17605, 2018.
- He Q, Wu KCH, Bennett AN, Fan B, Liu J, Huang R, Kong APS, Tian X, Kwok MKM and Chan KHK: Non-steroidal anti-inflammatory drug target gene associations with major depressive disorders: A mendelian randomisation study integrating GWAS, eQTL and mQTL data. *Pharmacogenomics J* 23: 95-104, 2023.
- Ferkingstad E, Sulem P, Atlason BA, Sveinbjornsson G, Magnusson MI, Styrismisdottir EL, Gunnarsdottir K, Helgason A, Oddsson A, Halldorsson BV, *et al*: Large-scale integration of the plasma proteome with genetics and disease. *Nat Genet* 53: 1712-1721, 2021.

23. Wu Y, Zeng J, Zhang F, Zhu Z, Qi T, Zheng Z, Lloyd-Jones LR, Marioni RE, Martin NG, Montgomery GW, *et al*: Integrative analysis of omics summary data reveals putative mechanisms underlying complex traits. *Nat Commun* 9: 918, 2018.
24. Laskar RS, Muller DC, Li P, Machiela MJ, Ye Y, Gaborieau V, Foll M, Hofmann JN, Colli L, Sampson JN, *et al*: Sex specific associations in genome wide association analysis of renal cell carcinoma. *Eur J Hum Genet* 27: 1589-1598, 2019.
25. Sun J, Zhao J, Jiang F, Wang L, Xiao Q, Han F, Chen J, Yuan S, Wei J, Larsson SC, *et al*: Identification of novel protein biomarkers and drug targets for colorectal cancer by integrating human plasma proteome with genome. *Genome Med* 15: 75, 2023.
26. Breen MS, Dobbyn A, Li Q, Roussos P, Hoffman GE, Stahl E, Chess A, Sklar P, Li JB, Devlin B and Buxbaum JD; CommonMind Consortium: Global landscape and genetic regulation of RNA editing in cortical samples from individuals with schizophrenia. *Nat Neurosci* 22: 1402-1412, 2019.
27. Lin J, Zhou J and Xu Y: Potential drug targets for multiple sclerosis identified through mendelian randomization analysis. *Brain* 146: 3364-3372, 2023.
28. Quinn PMJ, Moreira PI, Ambrósio AF and Alves CH: PINK1/PARKIN signalling in neurodegeneration and neuroinflammation. *Acta Neuropathol Commun* 8: 189, 2020.
29. Li Y, Chen H, Xie X, Yang B, Wang X, Zhang J, Qiao T, Guan J, Qiu Y, Huang YX, *et al*: PINK1-mediated mitophagy promotes oxidative phosphorylation and redox homeostasis to induce drug-tolerant persister cancer cells. *Cancer Res* 83: 398-413, 2023.
30. Zheng F, Zhong J, Chen K, Shi Y, Wang F, Wang S, Tang S, Yuan X, Shen Z, Tang S, *et al*: PINK1-PTEN axis promotes metastasis and chemoresistance in ovarian cancer via non-canonical pathway. *J Exp Clin Cancer Res* 42: 295, 2023.
31. Herzog SK and Fuqua SAW: ESR1 mutations and therapeutic resistance in metastatic breast cancer: Progress and remaining challenges. *Br J Cancer* 126: 174-186, 2022.
32. Brett JO, Spring LM, Bardia A and Wander SA: ESR1 mutation as an emerging clinical biomarker in metastatic hormone receptor-positive breast cancer. *Breast Cancer Res* 23: 85, 2021.
33. Lü J, Zhao Q, Ding X, Guo Y, Li Y, Xu Z, Li S, Wang Z, Shen L, Chen HW, *et al*: Cyclin D1 promotes secretion of pro-oncogenic immuno-miRNAs and piRNAs. *Clin Sci (Lond)* 134: 791-805, 2020.
34. Ko YA, Yi H, Qiu C, Huang S, Park J, Ledo N, Köttgen A, Li H, Rader DJ, Pack MA, *et al*: Genetic-variation-driven gene-expression changes highlight genes with important functions for kidney disease. *Am J Hum Genet* 100: 940-953, 2017.



Copyright © 2026 Gao et al. This work is licensed under a Creative Commons Attribution-NonCommercial-NoDerivatives 4.0 International (CC BY-NC-ND 4.0) License.